ELSEVIER

Journal of Nuclear Materials 274 (1999) 287–298

journal of nuclear materials

www.elsevier.nl/locate/jnucmat

Influence of high-dose Kr^+ irradiation on structural evolution and swelling of 16Cr–15Ni–3Mo–1Ti aging steel

V.V. Sagaradze [a], S.S. Lapin [a], M.A. Kirk [b,*], B.N. Goshchitskii [a]

[a] *Institute of Metal Physics Ural Division RAS, Ekaterinburg, 620219, Russian Federation*
[b] *Argonne National Laboratory, Argonne, IL 60439, USA*

Received 30 September 1998; accepted 26 February 1999

Abstract

Austenitic (16Cr–15Ni–3Mo–1Ti, 16Cr–15Ni–3Mo) stainless steels have been exposed to Kr^+ irradiation ($E = 1.5$ MeV, $T_{irr} = 500$–700°C, dose – up to 200 dpa) to compare with fast neutron irradiation ($E > 0.1$ MeV, $T_{irr} = 480$–500°C, dose – up to 60 dpa). Structural evolution, concentration changes and void formation were investigated. It was found that structural transformations in these steels are in qualitative agreement under Kr^+ and fast neutron irradiation. High resistance to swelling of aging stainless steel with 1% Ti is explained by the presence of both indirect point-defect sinks (γ' precipitates) and thermally stable direct dislocation sinks pinned by dispersed particles under irradiation.

1. Introduction

Sophistication of fast-neutron reactors and development of fusion reactors requires creation of alloys with a high resistance to radiation void-formation at temperatures of 400–700°C. A low radiation resistance of steel in fuel elements does not allow considerable burn up of nuclear fuel in fast neutron reactors. FCC austenitic steels are more prone to radiation void formation as compared to bcc ferritic steels. The latter are less resistant to corrosion, creep and embrittlement.

In the early 1970s, soon after radiation swelling was found [1], the main reasons for this phenomenon were explained and principal methods of swelling retardation were established [2–7]. Later studies greatly extended our understanding of the void formation and the structure evolution in various alloys subject to irradiation with high-energy particles [8–20].

Various approaches have been proposed to preclude vacancy swelling of austenitic steels:

1. Doping of stainless steels with small amounts (up to 0.5 mass%) of Ti or Si impurity to form vacancy-impurity complexes and to enhance recombination of point defects [8];
2. Preliminary cold deformation of alloys (up to ~30%) in order to greatly increase the number of point defect sinks (as edge dislocations) and to delay the onset of vacancy-void formation [7];
3. Radiation-induced precipitation of dispersed phases (intermetallics of $Ni_3Ti(Al)$ type) [6] to change the character of migration of point defects and to enhance their recombination. This phenomenon was observed for the first time in a high-nickel alloy – nimonic PE-16 [6];
4. Precipitation of plate phosphides under irradiation of stainless steels purposefully doped with phosphorus [9,10]. The influence of phosphide aging may be attributed to formation of small helium bubbles near the phosphides, the bubbles serving as neutral sinks of point defects;
5. A complete solution of the problem of swelling consists in replacement of fcc steels by bcc stainless steels, admitting impairment of corrosion and mechanical properties.

Today the goal of research is to bring the swelling resistance of fcc austenitic alloys to the value observed in bcc ferritic and ferritic–martensitic steels, while preserving the advantages of austenite. The austenitic

* Corresponding author. Fax: +1-630 252 4798

0022-3115/99/$ – see front matter
PII: S0022-3115(99)00090-2

materials that are most resistant to swelling are high-nickel precipitation-hardening fcc alloys [6,14]. However the alloys become highly brittle owing to the radiation-induced precipitation of a large amount of intermetallic phases, specifically $Ni_3Ti(Al)$ [14]. The recent investigations showed [18–20] that there is no need to add more than 40% nickel and 2–3% titanium or aluminum in the alloys. It is sufficient to introduce to high-purity ($\leqslant 0.02$ mass% C) stainless steels of the 16Cr–15Ni–3Mo type such an amount of titanium ($\sim$1 mass%) that would permit transforming a typical reactor steel to a precipitation-hardening steel subject to irradiation at 450–600°C.

The first experiments [18–20] performed on 16Cr–15Ni–3Mo–1Ti aging austenitic steel showed that its swelling is almost an order of magnitude lower ($\sim$0.6%) than swelling of an analogous steel containing 0.3% Ti when both steels were irradiated with fast neutrons at the energy $E > 0.1$ MeV and the most hazardous temperature of 480°C (dose of 60 dpa) in a commercial BN-600 reactor (Russian Federation). Dose and temperature dependencies of the radiation void formation were not measured for this steel. Therefore the first major task of this present research was to analyze the structural changes and to measure the temperature dependence of the vacancy void formation for the 16Cr–15Ni–3Mo–1Ti steel (in comparison to the titanium-less steel) under a high-dose (up to 200 dpa) ion irradiation. Ion irradiation of thin foils in situ a high-voltage electron microscope were performed to simulate neutron irradiations.

2. Materials, thermal treatment and methods

Steels of the following composition were produced in a vacuum induction furnace (mass%):

1. 16Cr–15Ni–3Mo–1Ti (15.9Cr; 15.0Ni; 2.5Mo; 1.02Ti; 0.03C as measured by chemical method);
2. 16Cr–15Ni–3Mo.

The steels were quenched from 1050°C and were found in a single-phase austenitic state. Neutron irradiation carried out at 480–500°C led to precipitation of up to 3% coherent ordered γ' phase of Ni_3Ti only in the steel with 1% titanium [18–20]. This was seen from appearance of superstructure reflections in neutron diffraction patterns [20].

Thin foils of proposed stainless steel containing 1% titanium and titanium-less steel of a similar composition were irradiated with Kr^+ ions directly in an electron microscope [21] or in an accelerator (followed by examination of the irradiated foils under a JEM-100CX microscope). A maximum irradiation dose of 200 dpa was sufficient to produce vacancy-voids in steels.

The 16Cr–15Ni–3Mo–1Ti austenitic steel was subject to ion irradiation after three different treatments: (a) after quenching from 1050°C; (b) after aging 8000 h at 650°C, which leads to coarsening of the precipitating phases and simulates long-time holding (up to $\sim$300 days, 60 dpa) in a neutron reactor (a high-dose (up to 200 dpa) irradiation with 1.5 MeV krypton ions requires less than 3 h); (c) after cold deformation with a reduction of $\sim$20%.

For swelling analysis the foil thickness was determined in a TEM from the extinction bands [22] under dynamical diffraction condition, or the inclined boundary of the grain in the $(2\ 0\ 0)_\gamma$ reflection. In most cases the foil thickness was $\sim$200 nm. A Philips CM-30 electron microscope with EDAX-9900 nano-probe was used to determine the concentration of elements in the foil (minimum size of the probe is 30 nm).

3. Choice of ion irradiation

To simulate fast neutron irradiation by ion irradiation a number of different ions and energies were investigated using an amended version of TRIM [23], which calculates the integral fractions of primary recoils and damage energy as a function of primary recoil energy. These recoil spectra could then be compared with the same spectra for irradiations by fast neutron spectrum. Whereas, in a very thin Fe TEM sample a reasonably good simulation recoil spectra for fast neutron irradiation would be with 400 keV Fe ions, to get sufficient dose (200 dpa) in a few hours required larger mass. The larger mass required higher ion energy to get sufficient transmission through a typical TEM sample thickness of 100 nm and thus fairly uniform damage through this thickness. Combining these with factor of accelerator reliability, the choice of irradiation was 1.5 MeV Kr ions. Fig. 1 shows a comparison of this ion irradiation in Fe–16%Cr–15%Ni–3%Mo with that of a fast neutron irradiation in Cu. Notice that the medians in the damage energy distributions are similar (60–70 keV recoil energy). However the ion irradiation has more damage energy in recoils at higher energies and a higher fraction of low recoil energy events. These spectral differences are not expected to make a significant difference in the development of irradiation produced microstructure at the rather high doses in this study. Using a Kinchin–Pease model in a TRIM calculation yields a dose of 1 dpa for 4×10^{14} ions/cm^2. A damage level of 200 dpa could be reached by an irradiation time 2–3 h.

However, other differences between this ion irradiation condition and a fast neutron irradiation must be considered. Recoil events from ion irradiation will be more correlated in space along each incident ion path, and the thin sample (100 nm) might provide a dominant sink structure (nearby surfaces) to distort the results. We feel neither is important at the high doses, and resultant high density of irradiation produced sink structures,

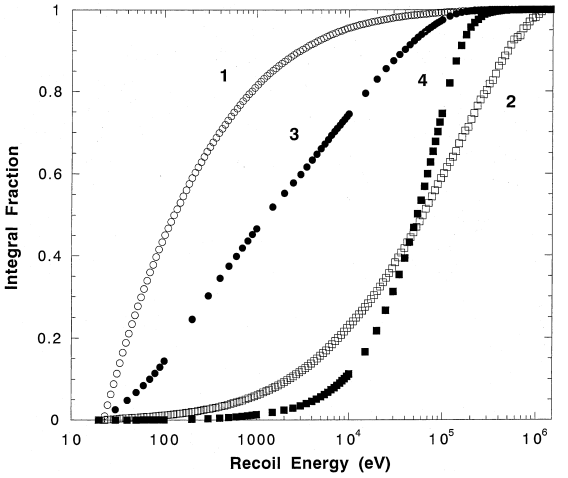

Fig. 1. Recoil (1,3) and damage (2,4) fraction under irradiation of steel 16Cr–15Ni–3Mo with K^+ ions (1,2) and under fast neutron irradiation of Cu (3,4).

used in this study. Two other differences which are undoubtedly more important are the greatly enhanced dose rate and the deposited Kr atoms. The latter amounts to about 1% of the ion dose in a 100 nm sample thickness. The dose rate is about 4 orders of magnitude higher for this ion irradiation than of a typical fast neutron irradiation in core. It is unknown at this time if the deposited Kr near the back surface of the foil has a significant effect on void nucleation and growth. However, the enhanced dose rate may be compensated by a shift in the peak temperature for swelling. Thus, results may be interpreted to apply to bulk neutron irradiations at lower temperatures.

4. Experimental results

4.1. Temperature dependence of swelling of 16Cr–15Ni–3Mo steels with and without titanium

Vacancy voids are formed during Kr^+ irradiation in the investigated steels. Fig. 2(a) shows size distribution of the voids in the steels depending on the temperature of irradiation with 1.5 MeV Kr^+ ions. Fig. 2(b) depicts the temperature dependence of vacancy swelling of the test stainless steels depending on their composition and thermal treatment. As is seen, the quenched steels with 1% Ti swell much less than the titanium-less steels (0.12% and 2.25%, respectively, irradiation temperature = 650°C). Subject to irradiation at 650°C (dose = 200 dpa), an average size of the voids is larger too, in the 16Cr–15Ni–3Mo steel (~14 nm) than in the same steel containing 1% Ti (3–4 nm). Very often the vacancy voids in Kr^+-irradiated steels were so small that

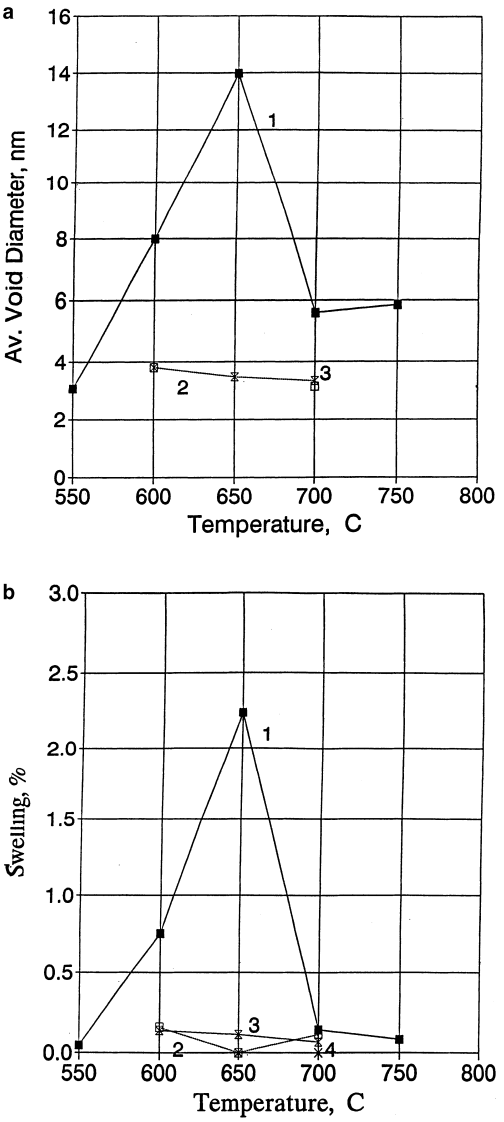

Fig. 2. Average size of voids (a) and vacancy swelling $\Delta V/V$; (b) in stainless steels depending on the temperature of irradiation with Kr^+ ions (dose = 200 dpa). (1) 16Cr–15Ni–3Mo steel quenched from 1050°C (■); (2) 16Cr–15Ni–3Mo–1Ti steel quenched from 1050°C (□); (3) 16Cr–15Ni–3Mo–1Ti steel quenched from 1050°C and aged at 650°C for 8000 h (⊠); (4) steel quenched and cold-deformation to 20% (X).

we had to detect them additionally by the change of the light contrast to the dark one during underfocusing and overfocusing in accordance with the technique described in [24]. Fig. 3(a) and (b) shows voids formed in the 16Cr–15Ni–3Mo steel after irradiation (200 dpa) at 650°C under conditions of underfocusing (a) and overfocusing (b). The void distribution is bimodal. There are large and small voids in titanium-less steels. Fig. 3(c) illustrates the small void size in austenitic steels with 1%

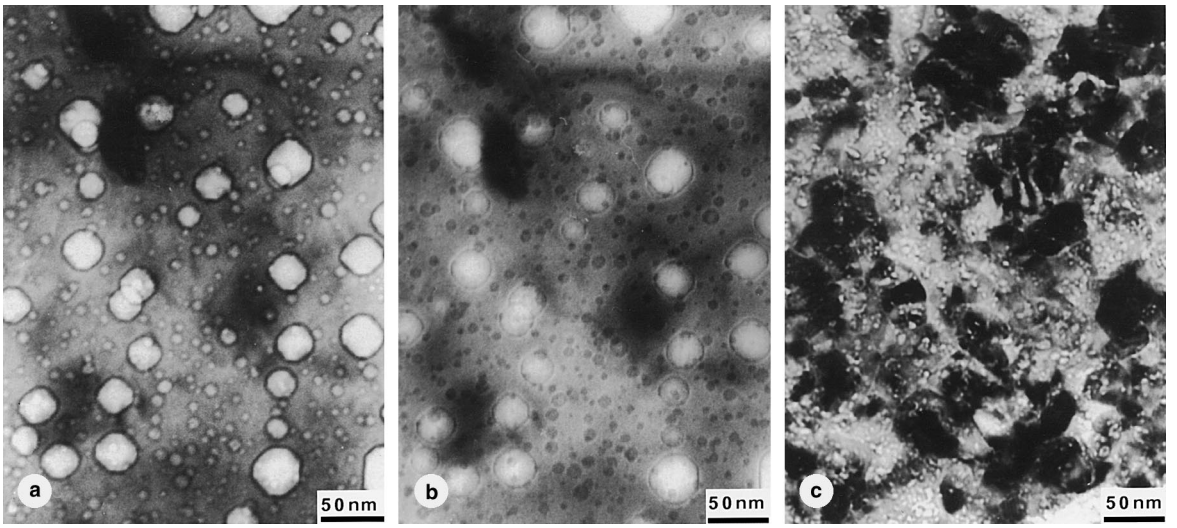

Fig. 3. Vacancy voids in the 16Cr–15Ni–3Mo (a,b) and 16Cr–15Ni–3Mo–1Ti (c) after irradiation with 1.5 MeV Kr^+ ions at 650°C (dose = 200 dpa); (a) underfocused; (b) overfocused.

titanium. The size difference becomes most pronounced under ion irradiation at 650°C.

Note specific features of the structural pattern of swelling arising under irradiation with fast neutrons ($E > 0.1$ MeV) and krypton ions with an energy of 1.5 MeV:

(1) When the 16Cr–15Ni–3Mo steel is irradiated with fast neutrons and Kr^+ ions, the temperature dependence of the vacancy swelling is shaped like a dome. In the case of ion irradiation the maximum on the $\Delta V/V = f(T)$ curve is shifted, as in [7,14], towards higher temperatures (from 500°C with fast neutron to 650°C for Kr ions).

(2) Generally vacancy voids formed under ion irradiation are much smaller than those produced under neutron irradiation. For example, voids with an average size of ~80–100 nm are formed in the 16Cr–15Ni–3Mo and 16Cr–15Ni–3Mo–1Ti steels [18–20] (see Fig. 4) when these are subject to neutron irradiation in the BN-600 reactor up to a dose of 60 dpa at 480°C. Irradiation of the same steels with Kr^+ ions even to higher doses (200 dpa) at the maximum swelling temperature of 650°C causes appearance of voids having an average size of 3–14 nm.

(3) A greater swelling of the steels with and without Ti under ion (Kr^+) irradiation is determined mainly by

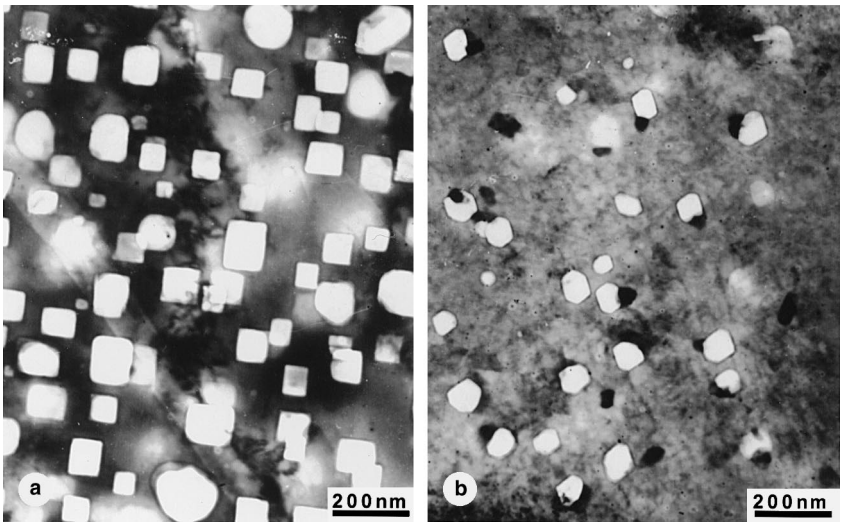

Fig. 4. Vacancy voids in the 16Cr–15Ni–3Mo–0.3Ti (a) and 16Cr–15Ni–3Mo–1Ti (b) steels after irradiation in the BN-600 reactor with fast neutrons at 500°C (dose = 60 dpa) [20].

an increase in the void size (cf. Figs. 2 and 3). Under neutron irradiation a rise in $\Delta V/V$ for different steels is determined by an increase in the density of voids, with their size being approximately equal: lowering of swelling $\Delta V/V$ of the Cr16Ni15Mo3 steel containing 1% Ti from 4.4%–0.6% is due to a decrease in the density of voids from 1.7×10^{20}–0.25×10^{20} m^{-3}, while an average size of the voids is approximately the same and equals 80 and 78 nm [20]. In other words, it was found that addition of 1% Ti to steels of the 16Cr–15Ni–3Mo type lowers the void nucleation rate under neutron irradiation (500°C) and decreases the void growth rate under ion irradiation (650°C, Kr^+ ions).

(4) Simulation irradiation with high-energy Kr^+ ions confirmed the fact that radiation void formation is largely retarded over the precipitation hardening range in quenched austenitic steels of the 16Cr–15Ni–3Mo type doped with 1% Ti. It is shown that the positive effect of 1% Ti persists over a rather broad temperature interval (500–700°C) up to high doses (200 dpa). Note that addition of 0.3–0.5% titanium, as is a common practice, is insufficient to suppress radiation swelling [18–20].

4.2. Structural evolution of the steels with an increase in the Kr^+ fluence

We did not pose ourselves the task to trace structural changes that occur in steels at early stages of irradiation (the onset of formation of Frank loops, their transformation, etc.). The main research was done after accumulation of large fluences (dose $\geqslant$ 10 dpa), which bring the Fe–Cr–Ni system closer to formation of radiation-induced voids. Fig. 5(a)–(c) shows the structure of the titanium-less 16Cr–15Ni–3Mo steel in the initial state (a) and after irradiation at 600°C up to 80 dpa (b) and

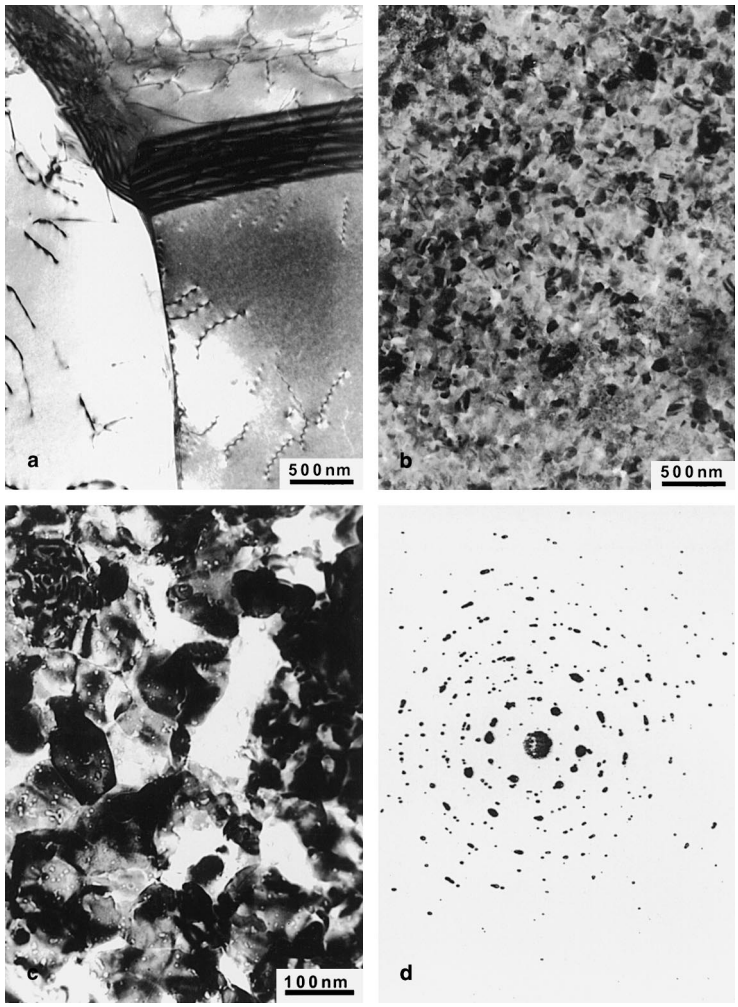

Fig. 5. Structure of the 16Cr–15Ni–3Mo steel in the initial state (a) and after irradiation with 1.5 MeV Kr^+ ions up to a dose (dpa) of 80 (b), 200 (c) at 600°C, (d) electron diffraction pattern at 200 dpa.

200 dpa (c). Even irradiation with krypton ions up to the dose of 10 dpa caused rearrangement of Frank loops to usual dislocations, which are largely transformed into subgrains at 600°C. The structure of the former grain comprises fine subgrains measuring 20–100 nm in size. A regular network of reflections from one grain after irradiation up to 10 dpa remains practically unchanged in the electron diffraction pattern. But part of reflections is smeared azimuthally and new point reflections appear near the initial reflections. This suggests formation of subgrains rotated to several degrees within the former austenite grain. As the irradiation dose is raised to 80–200 dpa, the subgrains grow a little. The subgrains formed under the dose of 200 dpa (600°C) are well seen at large magnification in Fig. 5(c). Electron diffraction pattern with zone axis [1 1 0] (Fig. 5(d)) show more azimuthal smearing of reflections (rotation of subgrains) and appearing of new reflections (formation of new grains). Some subgrains and small grains reach 100–150 nm in size, but there are fine entities measuring 20–40 nm. In addition to the developed subgrain structure, reflections from other phases are present. Probably, these are separate carbides, the Laves phase, σ, χ or G phases [14,16,17,25].

An increase in the irradiation temperature to 650°C leads to appearance of recrystallized grains, which absorb the γ-matrix with a dispersed substructure. Fine vacancy voids become more pronounced in the recrystallized grains. No marked changes in the concentration of the main alloying elements (Cr, Ni, Mo and Fe) were revealed when the concentration was measured using a EDS probe about 30 nm in size.

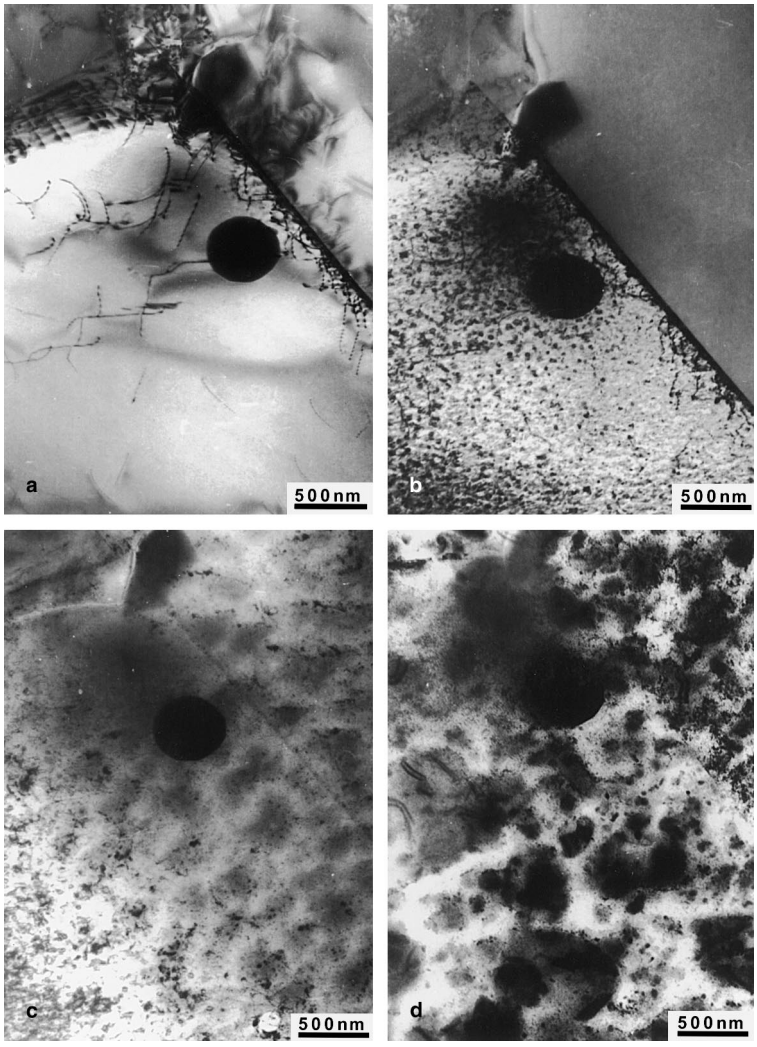

Fig. 6. Structural evolution of the 16Cr–15Ni–3Mo–1Ti steel irradiated with Kr^+ ions ($E = 1.5$ MeV) from 0 dpa (a) to 10 dpa (b), 30 dpa (c), and 200 dpa (d) at 550°C.

A different situation is observed in the steel containing 1% titanium. Figs. 6 and 7 illustrate the structural evolution of the 16Cr–15Ni–3Mo–1Ti steel during irradiation with Kr^+ ions ($E = 1.5$ MeV) to the dose of 200 dpa at 550°C. The principal distinction of the steel containing 1% Ti from the titanium-less steel is that the dislocation structure of the former offers a higher thermal and dose resistance. Even heating to 650°C (dose of 200 dpa) did not cause a breakdown of the γ grain into small subgrain constituents (Fig. 8).

Frank loops appear in regions free of dislocations (see the area near the spherical particle in Fig. 6(b), Fig. 7(b) and are preserved at the irradiation dose of 10 dpa (550°C). Note that some dislocations, which existed before irradiation, are preserved after irradiation to 10 dpa (see Figs. 6 and 7). Three dislocations changed somewhat their positions but dispersed particles (most probably, γ' phase) precipitated on dislocations in the aging steel. Particles about 10 nm in size are seen in Fig. 6(b) and the corresponding scheme in Fig. 7. If the irradiation dose is increased to 30 dpa (Fig. 6(c)), the structure starts to separate into alternating dark and light γ-constituents spaced 200–250 nm from one another and forming a mosaic pattern. Numerous dispersed particles and dislocations are observed inside this 'coarse separation'. Such a picture is preserved up to 100 dpa. The dark and light areas have the same orientation (as distinct from the subgrains in the titanium-less steel) and illuminate in the matrix reflection. An analogous contrast was found in irradiated Fe–35Ni and Fe–Cr–35Ni alloys [15] and attributed to a redistribution of the alloying elements (nickel, iron and chromium)or 'spinodal-like decomposition' under a high-temperature (400–800°C) irradiation. The authors [15] observed oscillations of the composition with a period of ~200 nm and explained alternation of the dark and light

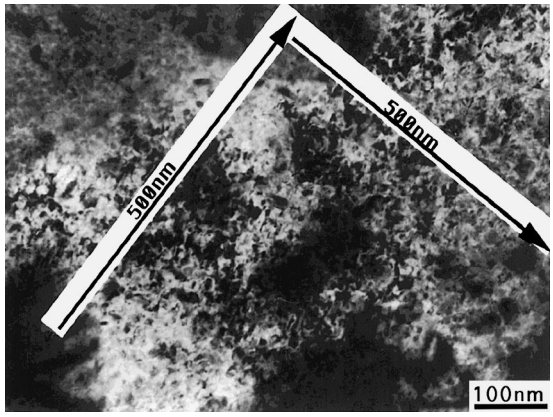

Fig. 8. Structure of the 16Cr–15Ni–3Mo–1Ti steel irradiated with 1.5 MeV Kr^+ ions up to a dose 200 dpa at 650°C. On arrow – way of EDS nano-probe.

contrasts by different etching of the γ regions containing different amounts of nickel. In our case the change of the contrast is not associated with different etching of foil portions (prior to irradiation the foil was homogeneous). Most probably, it is due to a different chemical composition of the precipitated regions and, possibly, to a different stress state of these regions. We observed [26,27] appearance of an analogous contrast in austenitic foils of the Fe–32 mass% Ni with local nickel redistribution.

As the irradiation dose is raised to 130 and 200 dpa (Fig. 6(d)), regions with more clearly defined boundaries of subgrains and particles appear inside the smeared dark-gray contrast. In the light-contrast regions fine particles and dislocations are observed also. According to [14,16,20,25], special carbides, γ' and η phases, Laves phases, χ, G and σ phases can be formed in stainless

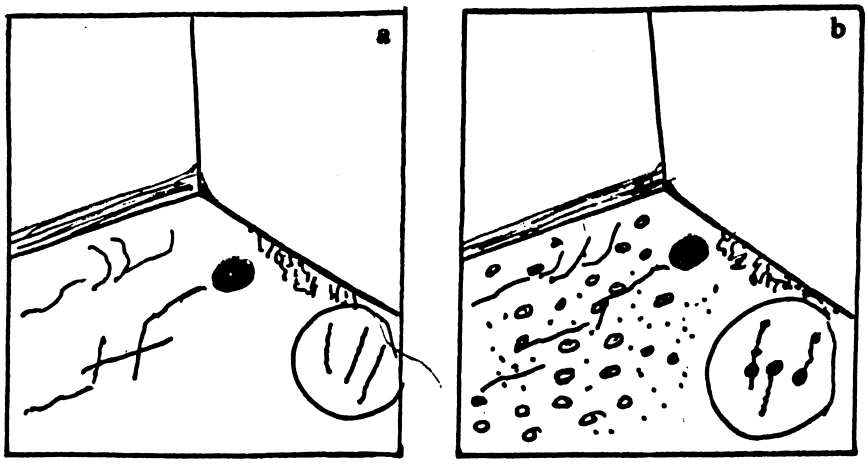

Fig. 7. Schematic sketch of three dislocations (encircled) in the 16Cr–15Ni–3Mo–1Ti steel before (a) and after (b) irradiation with 1.5 MeV Kr^+ ions up to a dose of 10 dpa at 550°C. Dislocation pinning particles are seen.

steels of a similar composition after a high-dose irradiation at elevated temperatures.

An increase in the irradiation temperature of the 16Cr–15Ni–3Mo–1Ti steel to 650°C incurs little qualitative changes in intragrain transformations. As the dose of irradiation with Kr^+ ions is raised the appearance of fine particles and dislocations is accompanied by formation of rather large dark regions up to 300 nm in size (Fig. 8). No recrystallization or polygonization is detected. An attempt was made to measure changes in the concentration of the alloying elements when the EDS probe (30 nm in diameter) passed from one particle to another. The probe movement diagram is given in Fig. 8. From the analysis it follows (Fig. 9) that the region accommodating an extended particle at the boundary with a twin contains seven times as high the amount of titanium as in the γ matrix (Fig. 9(a)). Changes with respect to the other elements in this region are insignificant. Note that owing to a little thickness of the particles the region in question is not limited to the particle and the probability of the probe getting to the matrix is high. For this reason the data on compositional changes should be treated only qualitatively. Considering that the amount of nickel in the region of this particle is not high, the particle has the composition of the TiC carbide rather than the Ni_3Ti intermetallic.

One more 'smeared' dark region located at a distance of about 300–400 nm from the first particle contains a high amount of chromium (~on 5 wt%) – see Fig. 9(b). Changes in the concentration of the other alloying elements (Fe, Si, Mo, Ni) in this chromium-enriched microregion represents an area of radiation-induced redistribution of elements or a zone of the initial formation of high-chromium phases (σ, δ ferrite). A detailed identification of these transformations calls for further investigations.

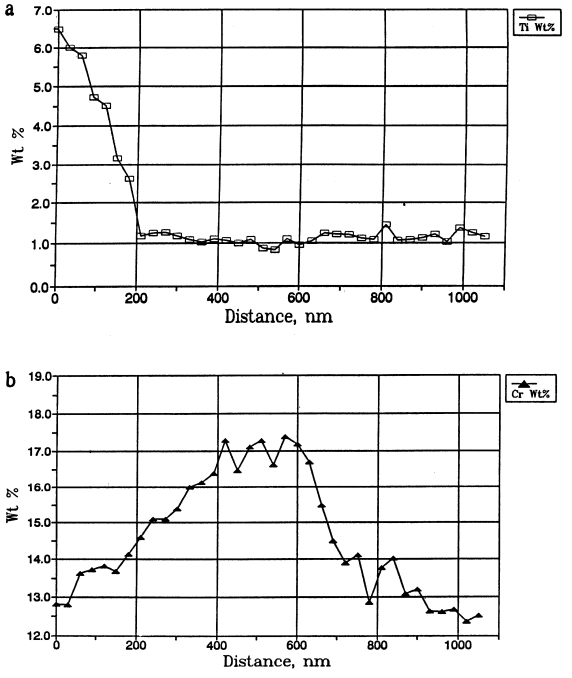

Fig. 9. Change in the concentration of Ti (a) and Cr (b) as the test probe moves from particle 1 to particle 2 (see the diagram in Fig. 8).

4.3. The effect of preliminary long-time aging

A significant point in ion and neutron irradiation is different time needed to accumulate the required dose. For example, irradiation of steel in the BN-600 fast-neutron reactor (Russian Federation) to 60 dpa requires about a year, while irradiation with 1.5 MeV Kr^+ ions at ANL (USA) to the same dose takes less than an hour. This difference in holding time at elevated temperatures can bring about absolutely different structural and phase transformations in the steels under study and, as a consequence, changes in the kinetics of void formation. To increase the time during which the 16Cr–15Ni–3Mo–1Ti aging austenitic steel is held at high temperatures, the steel was subject to a thermal aging at a temperature of 650°C for 8000 h outside the reactor. Under these conditions the processes of precipitation hardening proceed most intensively. Fig. 10(a) shows the structure of the aged 16Cr–15Ni–3Mo–1Ti steel, which was not irradiated. One can see precipitates of the ordered FCC γ' phase, which give superstructural reflections in electron diffraction patterns. An average size of the γ' particles on dark-field pattern is ~30 nm. Irradiation with Kr^+ ions up to a dose of 30 dpa has little if any influence on the shape and location of more coarse phases. The contrast from elastic distortions weakens ("arcs" disappear) near dispersed γ' particles, a fact which is probably connected with lowering of elastic distortions and partial loss of coherence between γ' phases and the γ matrix. The onset of precipitation of the alloying elements from the solid solution, which is determined by appearance of the alternating dark and white contrasts (as in the case of irradiation of the quenched steel), is observed after the irradiation dose of 30 dpa. Such mosaic dark–white contrast is most clearly seen after the doses of 80–160 dpa (Fig. 10(b)). At a large magnification (Fig. 10(b)) one can clearly see dispersed γ'-particles 20–30 nm in size located in light regions between coarse (200–500 nm in diameter) dark entities. So, during a high-dose irradiation the structural evolution of the preliminary aged 16Cr–15Ni–3Mo–1Ti steel differs little from the structural changes that take place in the quenched.

The void size (3–4 nm) and radiation-induced increase in the volume $\Delta V/V$ (0.1–0.2%) of the aged steel are also close to those of the quenched steel (see Fig. 2).

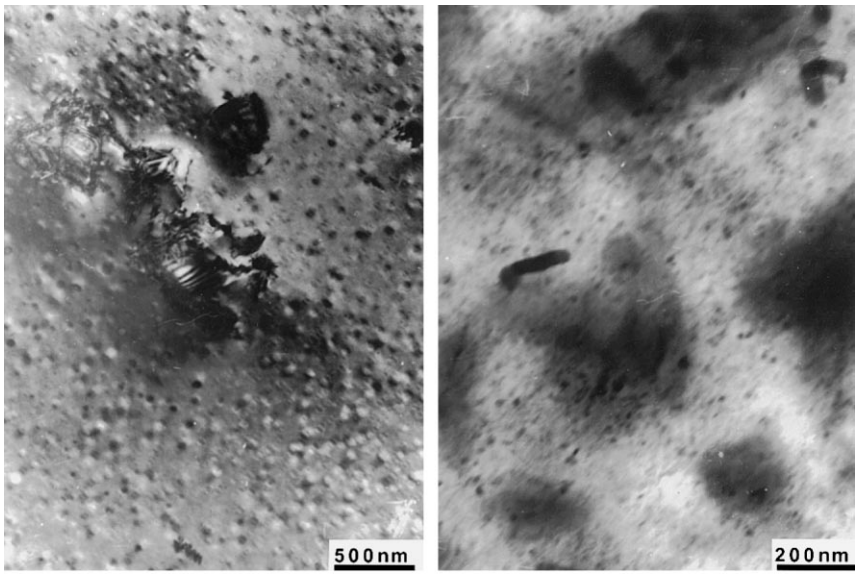

Fig. 10. Changes in the structure of the preliminary aged (650°C, 8000 h) 16Cr–15Ni–3Mo–1Ti steel irradiated with Kr^+ ions ($E = 1.5$ MeV, 650°C). Irradiation dose (dpa): a – 0; b – 160.

4.4. The effect of cold deformation

During reactor tests of steel of the 16Cr–15Ni–3Mo–1Ti type we failed to elucidate the simultaneous effect of high density of dislocations and numerous γ' precipitates on radiation swelling. As is known, a high density of point-defect sinks in the form of dislocations ($\rho \approx 10^{11}$ cm^{-2}) produced as a result of a 20–30% cold deformation considerably delays the onset of radiation swelling [7–14]. Therefore of great interest was the research concerned with ion irradiation of the cold-deformed aging 16Cr–15Ni–3Mo–1Ti steel. Fig. 11 shows changes in the structure of the 16Cr–15Ni–3Mo–1Ti steel after cold deformation by rolling to 20% and irradiation with Kr^+ ions at 700°C (dose of 200 dpa). After irradiation under the given conditions the steel retains a high density of dislocations (they are probably pinned by the γ' phase particles).

An examination of the foils revealed no vacancy voids of the radiation origin (after the dose of 200 dpa). The dislocation structure and deformation twins are preserved up to 700°C (Fig. 11(a)) despite a high irradiation dose (200 dpa). It is only in some portions of the foil that formation of fine recrystallized grains starts at 700°C (Fig. 11(b)). Particles of the γ' phase are clearly seen in these areas. This fact supports the supposition as to the increase in the vacancy swelling resistance under a simultaneous effect of γ' particles and high density of dislocations.

5. Discussion

5.1. On probable reasons for different effect of neutrons and Kr^+ ions

Let us consider probable reasons responsible for different effect that fast neutrons ($E > 0.1$ MeV) and Kr^+ ions with an energy ~1.5 MeV exert on void formation. First, recoil energy spectra of neutron and ion irradiations are different. The second reason may be different (10^4 times) rate of creating of dpa in fast neutron reactor or ion acceleration. It is known that the swelling peak of steels is shifted to high temperature region with increasing the damaging dose rate (e.g., neutrons) [14], because recombination conditions of point defects are altered. The maximum density of voids in the steel under neutron or ion (Ni) irradiation is reached at 480°C and 610°C, respectively [30]. In our case the austenitic steel is damaged by high-energy Kr^+ ions ~10^4 times faster than under neutron irradiation to the dose of 60 dpa. As a result, the swelling peak is shifted from 500–650°C (Fig. 2). The third probable reason is alloying of the foil with krypton atoms. Calculations made using the TRIM program showed that ~1% krypton atoms with an energy of 1.5 MeV may be retained in the foil 100 nm thick. If it is assumed that the total number of atoms in thetarget is 3×10^{16} (foil 100 nm thick and 2 mm in diameter), 2×10^{15} krypton ions hit the target (fluence of 6.8×10^{16} cm^{-2}) and 1% krypton atoms is left in the

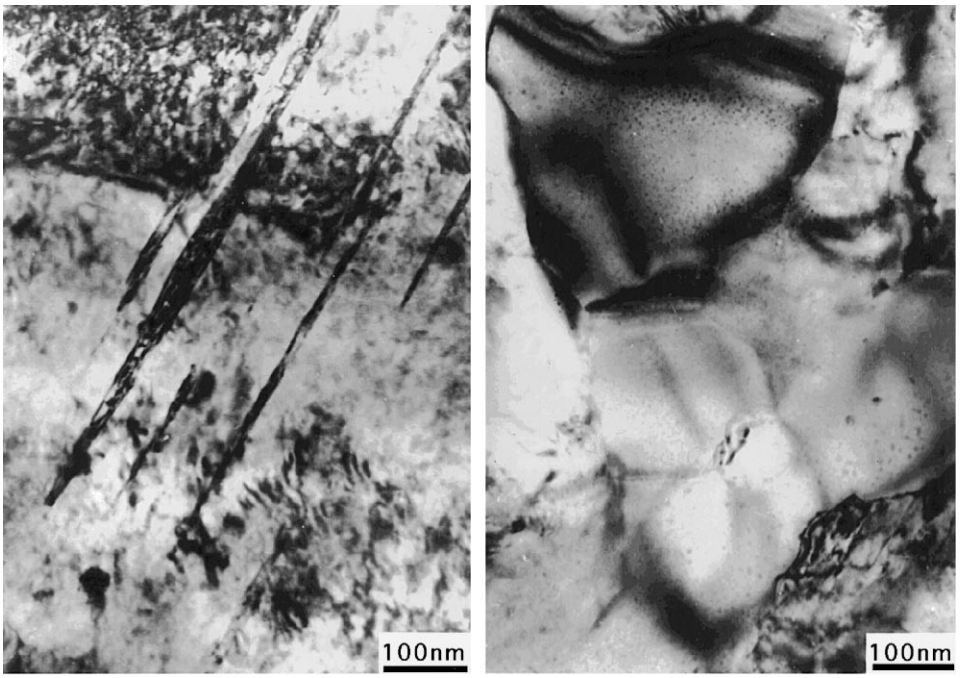

Fig. 11. Structure of the 16Cr–15Ni–3Mo–1Ti steel after cold deformation by rolling (20%) and irradiation with Kr^+ ions to a dose of 200 dpa at 700°C (a,b).

target, then the share of krypton atoms can be as high as ~0.07 at.%. This amount of Kr atoms can affect void formation. As is known [28], when 0.01 at.% argon – a substitutional element – is added, swelling of the 321 steel lowers from 3–4% to zero subject to bombardment with Ni^{6+} ions with an energy of 46.5 MeV up to a dose of 40 dpa at 600°C. On the contrary, addition of helium – an interstitial element – enhances swelling of the 316 steel [7]. Mobility of vacancies can also be affected by formation of 'vacancy-impurity atom' complexes [31] (Kr^+ in our case). This will influence the void formation. However high-dose irradiation of 16Cr–15Ni–3Mo–1Ti steel by 0.8 Mev iron ions at 773 K also does not result in the swelling, in spite of absence of the 'vacancy-atom Kr' complexes. Probably the change of point defects generation rate is the general factor of temperature shift of swelling peak.

5.2. On some reasons for delay in radiation swelling of 16Cr–15Ni–3Mo–1Ti steels

The main distinction of the steel with 1% Ti from steels of a similar class without titanium or with 0.3–0.5% Ti is tendency of the former to precipitation hardening (with precipitation of γ' phase of Ni_3Ti) under irradiation at 450–700°C [18–20].

The main cause of delay in swelling is considered to be [20] the participation of point defects in diffusive flow of substitutional elements (Ni, Ti, Fe) during a universal and uniform precipitation of dispersed particles of Ni_3Ti. Since the particles precipitate uniformly at a rather close distance to one another (every 8–15 nm), radiation vacancies, which add to diffusion of the elements, move to these small distances. All this promotes recombination of point defects and retards swelling. Since the γ' phase particles are small (5–10 nm) and grow slowly in a weakly aging steel containing 1% Ti, they may dissolve partially in displacement cascades [29]. Then the cascade irradiation (with neutrons and ions) facilitates both precipitation and dissolution of γ' particles. This prevents completion of the processes of aging and resumption of swelling. Taking into account that during diffusion of the substitutional elements by the vacancy mechanism point defects are capable of moving towards the nucleus of the Ni_3Ti phase (toward iron and chromium atoms forced from this region), particles of the γ'-phase may be called indirect sinks of point defects. The number and density of these γ' particles, as well as the number and distribution of edge dislocations determine resistance of the steel to radiation swelling. Calculations and experiments show [20] that a considerable delay in swelling can be provided if about 2–3 vol.% γ' phase of Ni_3Ti measuring 50–100 nm is formed in stainless steel 16–15 containing 1% titanium. A larger concentration of titanium may lead to heavy embrittlement of the steel subject to irradiation.

The investigations performed suggest one more reasonable cause why Ti has a positive effect on swelling. The structure of steels, where a sufficient amount of γ'-particles of Ni_3Ti precipitate under irradiation, is more stable than that of stainless steels without titanium or with a small amount (0.3%) of titanium. Ni_3Ti particles facilitate pinning of dislocations and are responsible for preservation of a high density of point-defect sinks even at high irradiation doses up to 200 dpa. In titanium-less steels (16Cr–15Ni–3Mo) dislocations readily move and rearrange themselves under irradiation, forming boundaries of rather coarse subgrains free of dislocations. Voids that nucleate in the bulk of the subgrains become capable of growing and lead to radiation swelling.

Strong concentration redistribution of alloying elements during high temperature irradiations are also reason for change of diffusion kinetic of point defects and void formations [13].

6. Conclusion

(1) It is shown that structural and phase transformations in stainless steels are in qualitative agreement when the steels undergo irradiation with Kr^+ ions (1.5 MeV) and fast neutrons (>0.1 MeV). The temperature dependence of radiation swelling of stainless steels of the 16Cr–15Ni–3Mo type subject to irradiation with Kr^+ ions (dose = 200 dpa) is dome-shaped, as in the case of neutron irradiation. However, under ion irradiation, the radiation swelling maximum ($\Delta V/V = 2.25\%$) is shifted towards higher temperatures (650°C) and vacancy-voids have a smaller size (6–14 nm at 600–750°C) and a smaller total volume. A certain difference in neutron and ion effects on void formation is explained by different dpa rates of the irradiating particles.

(2) High-dose irradiation of stainless steels containing 1% Ti causes formation of a 'dark–white' mosaic contrast, which is explained by 'redistribution' of the alloying elements (in particular, chromium) of the γ solid solution. Other phases of different fineness precipitate simultaneously.

(3) It is shown that 16Cr–15Ni–3Mo austenitic stainless steels with 1% titanium and forming the intermetallic γ' phase during irradiation possess a high resistance to radiation void formation ($\Delta V/V \leqslant 0.2\%$) over a wide temperature interval (500–700°C) and a broad range of Kr^+ irradiation doses (up to 200 dpa). A preliminary long-time intermetallic aging impairs little, if at all, resistance of the austenitic steel with 1% Ti to swelling. Preliminary cold rolling enhances resistance of the said aging steel to void formation.

A proposition is made that high resistance of aging stainless steels with 1% Ti to radiation swelling is due both to the presence of indirect point-defect sinks in the form of numerous γ' particles precipitating under irradiation and to thermally stable direct dislocation sinks pinned by the said dispersed particles.

Acknowledgements

The authors gratefully acknowledge financial support by the US Department of Energy, the Industrial Partnering Program with the Newly Independent States, NIS-IPP-ANL-011.

References

[1] C. Cawthorne, E. Fulton, Nature 216 (1967) 575.
[2] Pughs et al. (Eds.), Proceedings BNES Conference on Void Formed by Irradiation of Reactor Materials, 1971.
[3] J.W. Corbett, L.C. Ianniello (Eds.), Proceedings Albany Conference on Radiation-induced Voids in Metals, USA-EG Symposium Series, 1972.
[4] Proceedings Conference on Radiation on Substructure and Mechanical Properties of Metals and Alloys, ASTM STP 529, 1973.
[5] S. Pugh, J. Brit. Nucl. Energy Soc. 3 (1971) 159.
[6] W.G. Johnston, J.H. Rosolowski, A.M. Turkalo, T. Lauritzen, J. Nucl. Mater. 54 (1994) 24.
[7] W.G. Johnston, J.H. Rosolowski, A.M. Turkalo, T. Lauritzen, J. Nucl. Mater. 48 (1973) 330.
[8] F.A. Garner, W.G. Wolfer, J. Nucl. Mater. 102 (1981) 143.
[9] H. Kurishita, T. Miroga, H. Watanabe, N. Yoshida, H. Kayano, M.L. Hamilton, J. Nucl. Mater. 212–215 (1994) 519.
[10] I. Shibahara, N. Akasaka, S. Onose, H. Okada, S. J. Nucl. Mater. 212–215 (1994) 487.
[11] A.M. Parshin, Structure, Strength and radiation damageability of corrosion-resistant steels and alloys, Metallurgiya, Chelyabinsk, 1988, p. 655.
[12] J.F. Bates, R.W. Powell, J. Nucl. Mater. 102 (1981) 200.
[13] Y.V. Konobeev, S.I. Golubov, Proceedings Internal Conference On Radiation and Materials Science, Alushta, USSR, 22–25 May 1990 (Kharkov, 1991) vol. 10, pp. 142–171.
[14] F.A. Garner, B.R.T. Frost (Ed.), Irradiation performance of cladding and structural steels in liquid metal reactors, in: Book Nuclear Materials, Material Science and Technology, vol. 10, 1993, pp. 419–543.
[15] F.A. Garner, J.M. McCarthy, K.C. Russel, J.J. Hoyt, J. Nucl. Mater. 205 (1993) 411.
[16] P.J. Maziasz, J. Nucl. Mater. 169 (1989) 95.
[17] P.J. Maziasz, J. Nucl. Mater. 205 (1995) 118.
[18] V.V. Sagaradze, V.A. Pavlov, V.M. Alyabiev et al., Phys. Met. Metall. 65 (1988) 128.
[19] V.M. Alyabiev, V.G. Vologin, S.F. Dubinin, S.S. Lapin, V.D. Parhomenko, V.V. Sagaradze, Fiz. Met. Metalloved. 8 (1990) 142.
[20] V.V. Sagaradze, V.M. Nalesnik, S.S. Lapin, V.M. Alyabiev, J. Nucl. Mater. 202 (1993) 137.
[21] Taylor, J.R. Wallace, E.A. Ryan, A. Philippides, J.R. Wrobel, Nucl. Instrum. and Meth. 189 (1981) 211.

[22] P.B. Hirsh, A. Howie, R.B. Nicholson, D.W. Pashley, M.J Whelan, Electron Microscopy of Thin Crystals, Mir, Moscow, 1968, p. 574.
[23] J.P. Biersack, L.G. Haggmark, J. Nucl. Mater. 174 (1980) 257.
[24] J.W. Edington. Interpretation of Transmission Electron Micrographs, vol. 3, Philips, Cambridge, England, 1974, pp. 65–67.
[25] I.M. Neklyudov, V.N. Voevodin, J. Nucl. Mater. 212–215 (1994) 39.
[26] V.A. Shabashov, V.V. Sagaradze, E.E. Yurchikov, A.V. Saveleva, Fiz. Met. Metalloved. 44 (1977) 1060.
[27] V.V. Sagaradze, A.I. Uvarov, Strengthening of Austenitic Steels, Nauka, Moscow, 1989, p. 272.
[28] R.S. Nelson et al., J. Nucl. Mater. 58 (1975) 11.
[29] A.S. Bakai, N.M. Kirykin. Ques. Atom. Scien. A. Techn. 5 (Kharkov, USSR, 1983) p. 33.
[30] D. Gilbon, L. Naour, G. Didout, V. Levi, J. Nucl. Mater. 100 (1981) 253.
[31] R.L. Simons, Hulbert. in: F.A. Garner, J.S. Perrin (Eds.), Twelfth International Symposium on Effects of Radiation on Materials ASTM, Philadelphia, 1985, pp. 820–839.